ejpmr, 2020,7(9), 348-362

SJIF Impact Factor 6.222

EUROPEAN JOURNAL OF PHARMACEUTICAL AND MEDICAL RESEARCH

www.ejpmr.com

Research Article

ISSN 2394-3211

EJPMR

IN-VITRO ASSESSMENT OF CERIUM OXIDE NANOPARTICLES AS PROMISING DRUG-DELIVERY VEHICLES: INFLUENCE OF SURFACE FUNCTIONALIZATION

Aparna Datta[1]*, Deblina Majumder[2], Preetam Guha Ray[2], Sayantan Dasgupta[3], Siddharta Mukherjee[4] and Somenath Roy[2]

[1]School of Pharmacy, Sharda University, Knowledge Park III, Greater Noida 201310, Uttar Pradesh, India.
[2]CSIR-Central Glass and Ceramic Research Institute, 196, Raja S.C. Mullick Road, Kolkata 700032, West Bengal, India.
[3]Department of Biochemistry, NRS Medical College and Hospital, 138 A.J.C. Bose Road, Kolkata 700014, West Bengal, India.
[4]Department of Metallurgical and Material Engineering, Jadavpur University, 188, Raja S.C. Mullick Road, Kolkata 700032, West Bengal, India.

***Corresponding Author: Aparna Datta**

School of Pharmacy, Sharda University, Knowledge Park III, Greater Noida 201310, Uttar Pradesh, India.

Article Received on 06/07/2020 **Article Revised on 26/07/2020** **Article Accepted on 16/08/2020**

ABSTRACT

In search of alternative materials for potential use as a drug-delivery vehicle, or as a theranostic agent, we have investigated in-vitro biocompatibility of cerium oxide (CeO_2) nanoparticles, having inherent reactive oxygen species (ROS) modulating properties. Two primary concerns for injectable drug carriers, namely, hemo-compatibility and non-specific protein adsorption, have been addressed using pristine ceria, as well as CeO_2 nanoparticles with activated hydroxyl, amine or thiol functional groups. In addition, cytotoxicity studies have been performed in-vitro on human hepatocellular carcinoma (HepG2) cell line. Our studies suggest that the overall biocompatibility of cerium oxide is considerably superior to silica, the widely studied metal-oxide as a potential drug career. Cytotoxicity and hemolytic activity of CeO_2 can be further tuned by deploying appropriate surface functionalization strategies. Our studies revealed that grafting aminosilane moieties on the surface of nano-ceria significantly reduced hemolysis, to a value of mere 5%, for a particle concentration as high as 1000 µg/ml. Additionally, we have observed inherent cytotoxicity of CeO_2 for cancer cells. Such observation paves the way to potential utilization of cerium oxide nanoparticles, not only as a drug carrier but also as a pro-oxidant therapeutic agent for cancer.

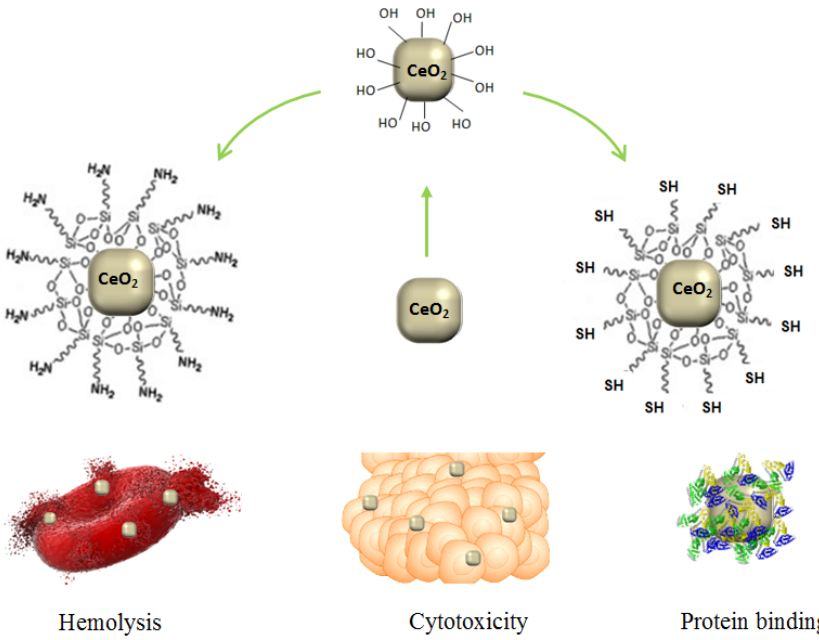

KEYWORDS: Cerium oxide; surface functionalization; hemolysis; cytotoxicity; protein adsorption.

1. INTRODUCTION

The emergence of nanotechnology has revolutionized the landscape of the pharmaceutical industry, with its prominent influence on the arena of targeted drug delivery. Controlled morphology, tunable surface properties, improved solubility, and multi-functionality of nanoparticles make them an attractive choice for developing intelligent nano-vehicles for therapeutic drugs. It has been demonstrated that nanocarriers tend to concentrate preferentially in solid tumor tissues due to the enhanced permeability and retention (EPR) effect of the vasculature.[1] Hence, nanoparticle-based cargos are especially suitable for targeted delivery of chemotherapeutic drugs.

Of late, oxide nanostructures, especially mesoporous silica nanoparticles (MSN), have shown promises as drug delivery vehicles, thanks to their tunable mesoporous structures that facilitate loading of therapeutic molecules, their retention through systemic circulation and subsequent controlled release at the target sites. Ever since the Mobil researchers synthesized mesoporous silica-based nanomaterial, codenamed as MCM-41,[2] their efficacies for optimal loading and controlled release of therapeutic cargos have been extensively investigated. For example, Vallet-Regi et al. studied the viability of this material as a drug delivery system by loading Ibuprofen into the pores at a drug-to-MCM-41 weight ratio of approximately 3:7.[3] These loaded MCM-41 particles were then subjected to a simulated body fluid and determined to be potentially viable drug delivery systems. This work demonstrated that mesoporous silica materials could be used to deliver relatively large doses of drug in a controlled manner. The drug delivery characteristics of mesoporous materials have also been modified via reversible capping of the surface pores. For stimuli-responsive release of neurotransmitters and drugs, Lai et al. developed chemically cleavable cadmium sulfide (CdS) nanoparticle caps attached to mesopores MCM-41 scaffold.[4] Though MSN has been studied most wisely as targeted drug delivery vehicle, some reports highlight the potential toxicity of MSN, primarily due to the interactions of surface silanol moieties with cellular membranes.[5] Hence, besides tweaking the surface chemistry of MSN, to reduce the cytotoxicity effect, it is worth exploring other metal-oxide nanostructures, for example, titanium dioxide (TiO_2) or cerium oxide (CeO_2), which have shown minimal signs of cytotoxicity.[6]

Nanocrystalline cerium oxide, owing to its unique physico–chemical properties, finds a gamut of applications in diversified fields such as histochemistry[7] electrolytes for solid oxide fuel cells,[8] ultraviolet absorbents,[9] oxygen sensors[10] and so on. Of late, the attention is eventually shifting to medical applications of nano-ceria, primarily owing to their radical scavenging capabilities to modulate oxidative stress in biological systems. For example, Xia et al. reported that internalized CeO_2 particles exert a cytoprotective effect due to its antioxidant properties.[11] Additionally, CeO_2-NPs are shown to attenuate myocardial oxidative stress and inflammatory processes in transgenic mice model.[12] Auto-catalytic anti-oxidant behavior of CeO_2 nanoparticles for ameliorating diseases of the central nervous system, including spinal cord repair, has been demonstrated in an in vitro model of rat spinal cord cells.[13] Further, in a study performed by Linse *et al.*, ceria nanoparticles seemed to act as nucleation site for protein fibrils from β_2-microglobulin.[14] This phenomenon mimics the amyloid formation mechanism involved in Alzheimer's and Creutzfeld-Jacob's disease. The wealth of background information about the cytoprotective activities of cerium oxide motivated us to conduct preliminary assessment of this material for its potential use as drug delivery vehicle.

2. MATERIALS AND METHODS

2.1 Materials

Cerium ammonium nitrate (≥ 97% pure), cetyltrimethylammonium bromide (CTAB), diethyl ether, ethylene glycol, ammonium hydroxide, and ethyl alcohol were obtained from Merck (India) and used as such without further purification. Polyvinylpyrollidone (PVP) was obtained from Loba cheme. India. Tetraethyl orthosilicate (TEOS), amphotericin B, 3-(4,5-Dimethyl-2-thiazolyl)-2,5-diphenyl-2H-tetrazolium bromide (MTT) and dimethyl sulfoxide (DMSO) were obtained from Sigma Aldrich. Trypsin-EDTA (in Hank's balanced salt solution, 0.25% Trypsin and 1mM EDTA, without Ca^{2+} and Mg^{2+}) was purchased from Merck Millipore Corporation. Sterile phosphate buffer solution (PBS 1M, pH 7.4), 3-mercaptopropyl-trimethoxysilane (MPTMS, 95% pure), (3-aminopropyl) triethoxysilane (APTES, ≥ 98% pure), Human Serum Albumin (fatty acid free) and Tetraethylorthosilicate (TEOS, ≥ 99% pure) were procured from Sigma Aldrich (Germany) and were used without further purification. Dulbecco's Modified Eagle's Medium (DMEM), heat-inactivated fetal bovine serum (FBS) and Penicillin-Streptomycin-Glutamine (100x) were purchased from Life Technologies (Thermo Fisher Scientific Inc.). Trypsin-EDTA (in Hank's balanced salt solution, 0.25% Trypsin and 1mM EDTA, without Ca^{2+} and Mg^{2+}) was purchased from Merck Millipore Corporation. HepG2 cells were obtained from National Centre for Cell Sciences (NCCS), Pune, India. All the reagents for the experiment were directly used after purchase and the water was Milli Q (Millipore, Beillerca, MA) as per the requirement. Aqua regia solution (HCl : HNO_3 = 3:1) was used to clean all the glassware prior to the synthesis of nanoparticles.

2.2 METHODS

2.2.1 Synthesis of ceria nanoparticles

Cerium ammonium nitrate as precursor (8 mM) and ploy vinyl pyrollidone (0.16 M) were vigorously stirred in 30 ml ethylene glycol to obtain a homogeneous colorless solution. This mixture was heated under reflux to 190 ^{O}C for 4 h. The color of the solution changed

initially to yellowish brown and brown gas was evolved. Eventually, the reacting solution turned milky and a white precipitate was obtained after stirring for 2 h. This precipitate was centrifuged and washed with DI water and ethanol several times to remove the excess reagents and then dried overnight in a vacuum oven at 80 ^{O}C. It was further calcined at 600 ^{O}C for 6 h to obtain pristine ceria nanoparticles (CeO_2).

2.2.2 Synthesis of silica nanospeheres

20 ml diethyl ether was mixed thoroughly with 70 ml DI water and 0.8 ml ammonia solution, in which 0.5 g of CTAB was dissolved and stirred for 30 min at room temperature. Subsequently, 2.5 ml of TEOS was promptly added into the mixture under continuous stirring. The stirring continued for 4 h at room temperature for the hydrolysis reaction to occur. The precipitate was washed with DI water several times and then dried at 60º C for 24 h. Calcination in air at 600 ºC for 5 h was done to remove the remaining surfactants, resulting in the formation of pristine silica nanoparticles (SiO_2).

2.2.3 Functionalization of ceria nanoparticles

Hydroxylated ceria: Water and ethanol was mixed in 1:1 ratio and to this mixture 0.3g of ceria nanoparticles (calcined at 600 ^{O}C for 6 h) was dispersed and ammonium hydroxide was added drop by drop with constant stirring until pH 8-9 was attained. The mixture was heated at 50 ^{O}C for 30 min to evaporate ethanol. 10 ml of 30% H_2O_2 was then added drop-wise and the mixture was kept at room temperature for 24 h. It was then heated at 50 ^{O}C for 1 h with constant stirring at 650 rpm. The sample was then centrifuged and dried at room temperature to obtain a powder termed as hydroxylated ceria (OH-CeO_2).

Amine-modified ceria: 0.2 g of OH-CeO_2 powder was dispersed in 10 ml ethanol and aged for 2 h. Subsequently, 1 ml of APTES was added and sonicated for 20 min in a bath sonicator and centrifuged. The collected precipitate was dried at room temperature, which hereinafter is called amine-modified ceria (NH-CeO_2).

Thiol-modified ceria: 0.3 g of OH-CeO_2 was added to 5 ml of DI water, to which ethanol was added drop-wise under constant stirring at 60 ^{O}C. 200 µl of MPTMS was then added to the solution and stirred for another hour at constant temperature along with the addition of ethanol. The slurry so obtained was then heated to evaporation until a dry powder was obtained, termed as thiolated (SH-CeO_2) ceria henceforth.

2.2.4 Hemolysis assay

Hemolysis experiments were carried out in triplicate on 36 healthy volunteers, approximately weighing 65-70Kg, upon obtaining their consents. Assays were performed following a procedure described in the literature with some modifications.[18] In the experimental process, 3 ml of blood sample was drawn aseptically from healthy volunteers, upon their consent, by a qualified professional at N.R.S. Medical College and Hospital, Kolkata. The collected blood samples were placed in lithium heparin as anti-coagulating agent containing BD Vacutainer® blood collection tubes. The sampled whole blood underwent centrifugation at 1600 rpm for 5 min, for segregation of RBCs. Subsequently, the plasma containing other blood components was decanted. The RBCs so obtained were washed 5 times with 6 ml PBS (pH 7.4) and to finish re-suspended in 25 ml of sterile isotonic PBS. This RBC suspension (0.2 ml) was mixed with varying concentrations (50 µg/ml – 1000 µg/ml) of pristine or functionalized nanoparticles suspensions in sterile isotonic PBS (0.8 ml). To prepare negative control, 0.2 ml of RBC suspension was added to 0.8 ml of sterile PBS whereas positive control was made by adding equal quantity of water instead of PBS. The samples and controls were incubated at 37 °C for 2 h following a gentle vortex. The samples were shaken at 30 min intervals to preclude precipitation of blood cells and nanoparticles. At the end of 2 h, the samples were centrifuged at 1600 rpm for 5 min. From each sample vial, 100 µl of supernatant was transferred to a 96-well plate in triplicate and absorbance of hemoglobin in the supernatants was measured with a micro plate reader at 570 nm. Hemolysis percentages of the RBCs were calculated using the following formula:[19]

% Hemolysis = (absorbance of sample – absorbance of negative control) / (absorbance of positive control – absorbance of negative control)

2.2.5 Cell Culture and viability assay

In this study, Human hepatoma HepG2 cells were used, which retain normal cell functions and have been used in a number of cytotoxicity studies. HepG2 cells (ATCC HB-8065), obtained from NCCS, Pune, India were maintained at 37 ^{O}C in Corning® plastic culture flasks in an atmosphere of 5% CO_2 and 95% humidified air. The culture medium consisted of DMEM, supplemented with 10% FBS, 4% Penicillin-Streptomycin-Glutamine and 5% fungicide (Amphotericin B). Cells were grown to 70 % confluence in 60 mm culture dishes.[20] These HepG2 cells were plated at a cell count of 105 cells/ml in a 96 well plate for cytotoxicity study using MTT assay, and allowed to attach for 24 hours prior to the addition of nano crystalline ceria. On the other hand, bare and surface modified nanoceria at different concentrations (50 µg/ml – 1000 µg/ml) were dispersed in cell culture media and aged for 24 hours before being added to the cells. For viability testing HepG2 cells were exposed in triplicate for 24, 48, 72 and 144 h to varied concentrations of ceria and surface modified ceria nanoparticles for concentrations 50 µg/ml, 100 µg/ml, 250 µg/ml, 500 µg/ml and 1000 µg/ml in 24-well plates at a cell count of 105 cells per well. The cytotoxicity of CeO_2 nanoparticles was evaluated by standard MTT assay. MTT was dissolved in sterile PBS at room temperature at 5 mg/ml, filtered to remove the insoluble

residue and sterilized, stored in a dark coloured bottle at 4 ^{O}C as stock solution. To each well of a 96 well flat bottomed plate, MTT (from stock solution) (10 µl per 100 µl medium) was added and given to rest for 2 hours at 37 ^{O}C. After treatment for stipulated time, the wells were washed with PBS (to rule out the interference from MTT interacts with CeO_2 nanoparticles in the suspension),[21] the medium was replaced with 100 µl of fresh medium. Dimethysulfoxide was added to all wells and mixed thoroughly to dissolve the purple crystals. The intensity of the purple color is comparative to the metabolic activity of the cell. Here, the study was made with amine-functionalized ceria and an evaluation was made with pristine CeO_2. We chose to go ahead with NH_2-CeO_2 owing to the fact that the presence of organosilane monomers on nano ceria particles was found to appreciably reduce their hemolytic activity. Nanoparticles-free media when added to HepG2 cells served as a control. The purple formazan crystals formed by dehydrogenase enzyme in live cells were dissolved with dimethyl sulfoxide and the optical absorbance at 570 nm was recorded by a microplate reader (model: AM 2100 from Alere Inc., Waltham, MA, USA).

The relative cell viability (%) = (absorption of a specific nanoparticles-treated well) / (absorption of control well) × 100%

2.2.6 Protein adsorption

HSA adsorption study was made following a recent report by Qianjun He et al.[22] Protein concentration (600 µg/ml) was kept invariable throughout the study while NPs concentration varied from 50 to 1000 µg/mL. The reaction mixture was first equilibrated at room temperature for 1hr and then UV-vis and fluorescence spectra were recorded to monitor the interaction of NPs with HSA. For our experiment, in 500 ml of DI water, 0.3 g of HSA was completely dissolved under constant shaking. This solution was stored at a temperature of 4 °C. Keeping the concentration of the protein constant varying concentrations (50, 100, 250, 500, 1000 µg/ml) of the nanoparticles were dispersed into 10 ml of PBS at a fixed temperature of 37 °C and a shaking rate of 150 rpm. To each of these nanoparticles suspensions, 5 ml of HSA was added. After 2 h of standing time, the mixed solutions were centrifuged and then upper clear solutions were collected. HSA adsorbed on ceria and the functionalized nanoparticles were calculated using following equation:

$$q = (Ci–Cf)\ V/m,$$

Where, Ci = initial HSA (0.2 mg /ml) concentration before HSA adsorption

Cf = final HSA concentration in solutions and after HSA adsorption

V = total volume of the solution (15 ml)

m = is the weight of NPs added into the solution

2.2.7 Characterization of the nanoparticles

The morphology of the synthesized cerium oxide nanoparticles was investigated using JEOL JEM 2100 high-resolution transmission electron microscope (HRTEM, JEOL USA, Inc., MA, USA). The samples were pre-treated at 300 °C for 2 h in vacuum. The nitrogen adsorption and desorption isotherms at 77 K were calculated using an Autosorb iQ automated gas sorption analyzer system (Quantachrome Corporation, FL, USA). The data analysis was performed using Quantachrome NOVA Win software version 10.01. The overall surface charge of the nanoparticles in solution (~1 mg/ml in DI water) at pH 7.4 (physiological condition), zeta potential (ζ), was assessed by Zetasizer Nano-ZS zeta potential analyzer (Malvern Instruments Ltd, Malvern, UK). Fourier-transform infrared spectroscopy (FTIR) using IRPrestige-21 FTIR spectrometer from Shimadzu Corporation (Tokyo, Japan) was used to check the presence of reactive moieties on the modified metal-oxide surface. Optical absorption measurements of the released hemoglobin, due to hemolysis caused by of nanoparticles, were carried out using Alere AM 2100 microplate reader (Alere Inc., Ontario, Canada). X-Ray Diffractometer (RigakuUltima III) determined the phase analysis of the nanoparticles prepared, carried out by with CuKα radiation (λ = 0.15418 nm) in a continuous scan mode from 20 ^{O}C to 80 ^{O}C at a scan speed of 1 degree / minute. Optical density for the MTT assay was done at 570 nm in a microplate reader (model 550, Bio Rad). The interaction at different concentrations (50 µg/ml – 1000 µg/ml) between bare and functionalized cerium oxide nanoparticles and HSA were determined after incubating the nano-crystal suspension with the protein solution at 600 µg/ml for 2 hours and then UV analyzing the supernatant at 279 nm by using a Shimadzu UV-3101PC spectrophotometer.

3. RESULTS AND DISCUSSION

3.1 Morphology and crystallography of the nanoparticles

Morphology of the synthesized cerium oxide, as investigated by TEM, is presented in Fig. 1(a). Well-dispersed individual CeO_2 nanoparticles, with a mean diameter of 90 nm, could be observed on the TEM grid [Fig. S1]. The SAED pattern, presented in Fig. 1(b) suggests some degree of polycrystallinity of the material. A closer observation from the high resolution TEM (HRTEM) image in Fig. 1(c) shows the presence of lattice fringes with d(111) = 0.31 nm, which corresponds to fast Fourier transform (FFT) image (inset). In Fig. 1(d), the EDAX result confirmed the absence of any impurities in the CeO_2 material. This indeed is very important to check the elemental level purity before any biological application. Besides morphological characterizations, it is apparent to discuss the formation mechanism where PVP, used as a surfactant, plays a significant role behind the formation of spherical CeO_2 nanoparticles. When Cerium ammonium nitrate is vigorously mixed with ethylene glycol in the reaction mixture, the intermediate cerium glycolate is formed. It initiates a nucleation process which may result larger particles due to aggregation and nearer spatial distance. The assembled aggregation of the intermediates are

minimized by the preferential interaction of PVP molecules with (100) plane of CeO_2 crystals. This eventually results in the growth of (111) plane, supported by both XRD and HRTEM. Polyvinylpyrrolidone also reduces the surface tension of the reaction mixture which may increase the Brownian motion of the particles rapidly and results in well dispersed CeO_2 nanoparticles.

Further, the crystallographic characteristics of the calcined CeO_2 nanomaterials were investigated by X-ray diffraction. The obtained diffraction peaks in Fig. 2(a) were consistent with the JCPDS card (No. 34-0394) for CeO_2 with a face-centered cubic structure and could be assigned to this structure. There absence of any other diffraction peak indicated high purity of the synthesized products. Calculations with the Debye–Scherrer formula, $d = \kappa\lambda/\beta\ (\cos\theta)$, for the peak with highest intensity (111), gave an average crystallite size of 10.7 nm. Here, κ is a constant equal to 0.89, λ is the X-ray wavelength equal to 0.154 nm, β is the full width at half maximum, and θ is the half diffraction angle.

Figure legends

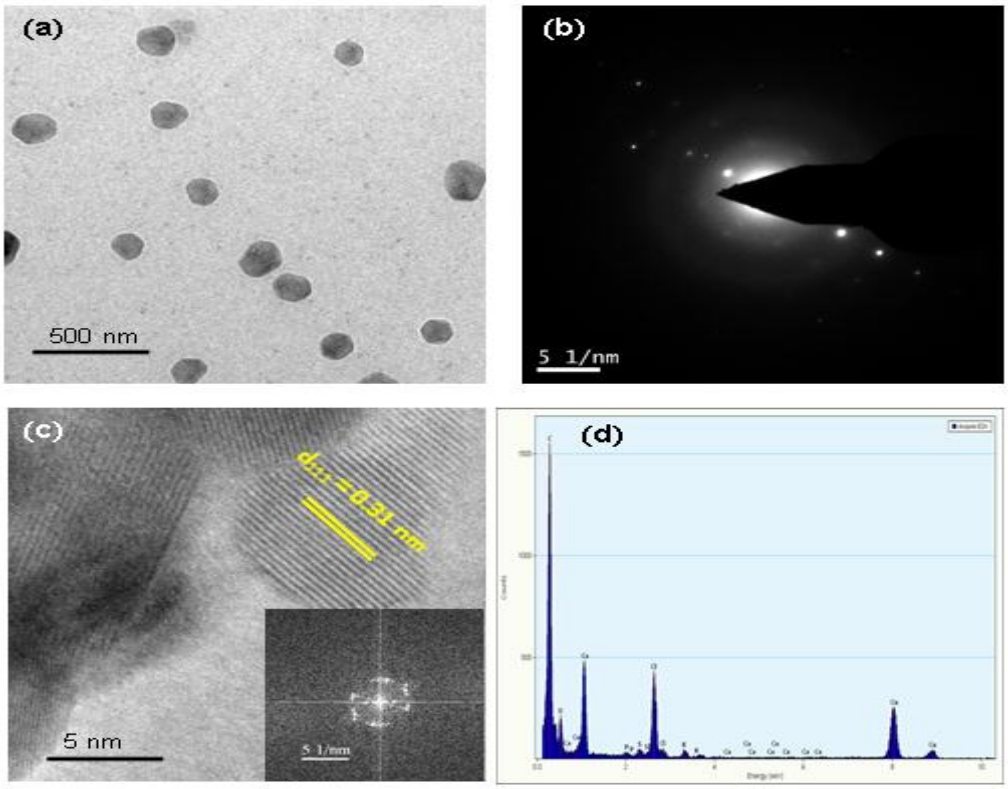

Fig. 1: (a) TEM image of the CeO_2 nanoparticles; (b) SAED pattern of the nanoparticles, (c) HRTEM image of the spherical nanoparticles, Inset: corresponding FFT pattern, (d) EDAX analysis of the nanomaterial.

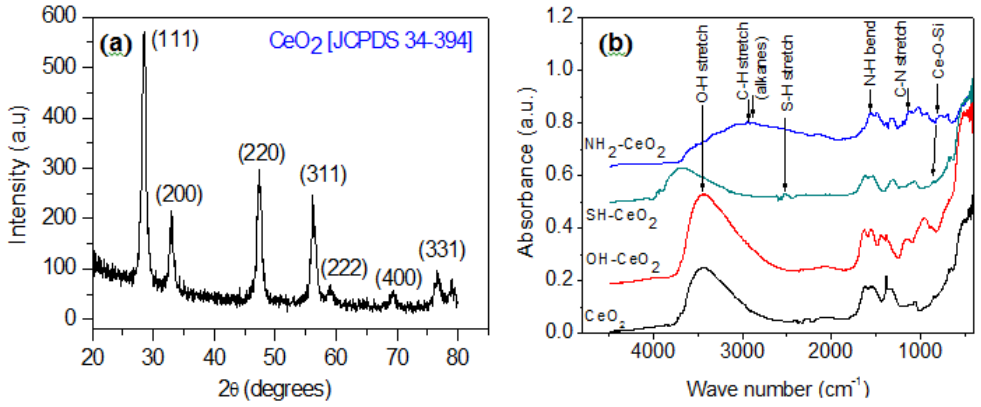

Fig. 2: (a) X-ray diffraction spectra for CeO_2 nanoparticles. Manifestation of the {111} plane is apparent from the relative intensities of the XRD peaks; (b) FTIR spectra of the pristine and surface functionalized CeO_2 nanoparticles. Chemical footprints of the functional moieties on the CeO_2 surface could be obtained from the respective absorption peaks or bands.

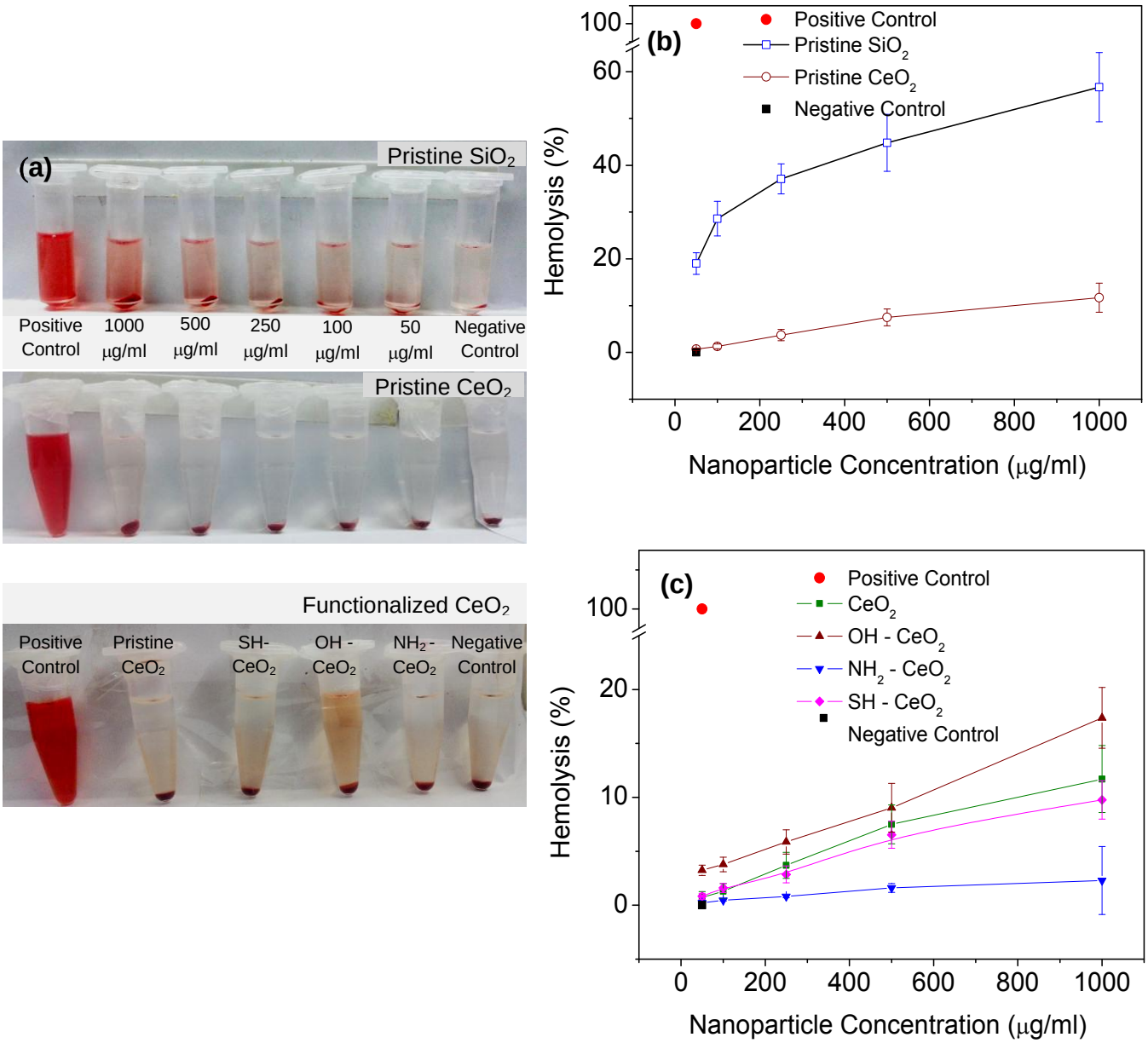

Fig. 3: Hemolysis assays for pristine and functionalized CeO_2 nanoparticles. (a) Three panels stacked vertically represent photographs of suspended RBCs treated with SiO_2 nanospheres, pristine CeO_2 and surface-functionalized CeO_2 nanoparticles, respectively. In case of functionalized CeO_2, the concentration of is 1000 µg/ml. The released hemoglobin from the damaged cells in the supernatant can be seen from the photographs. +ve and -ve controls are the RBCs in water and PBS, respectively, without exposure to the nanomaterials. (b) Hemolysis percentages of the CeO_2 nanoparticles as compared to SiO_2 nanospheres at different concentrations between 50 and 1000 µg/ml, which were incubated with RBCs at 37 ^oC for 2 h. (c) Degree of hemolysis caused by pristine and surface functionalized TiO_2 nanoparticles at different concentrations. Data generated from three independent experiments.

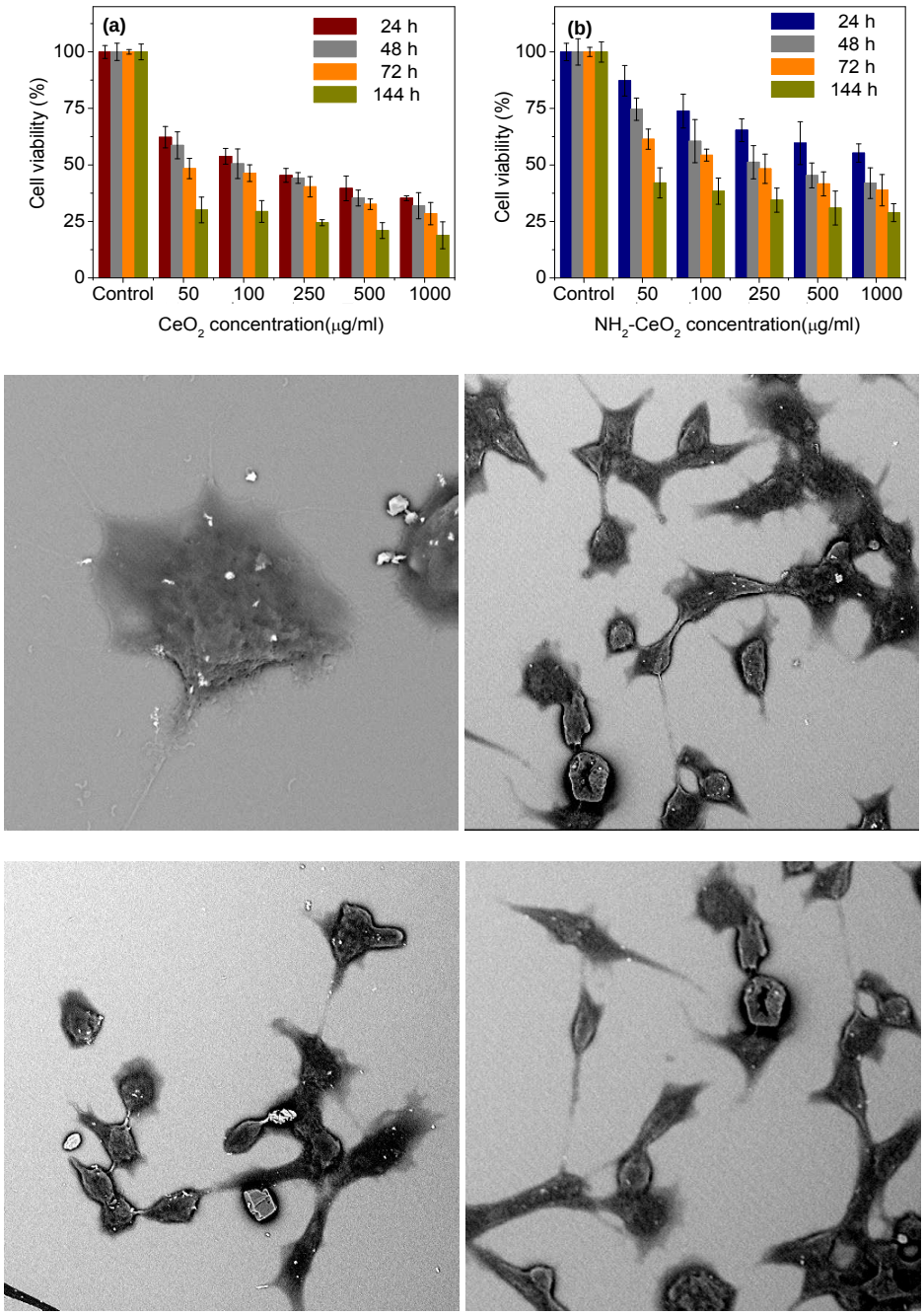

Fig. 4: Cytotoxicity of pristine and surface-modified CeO_2 nanoparticles. MTT assays after incubating the HepG2 cells with various concentrations of (a) pristine CeO_2 and (b) NH_2-CeO_2 nanoparticles for 24-144 h. (c) SEM image of pristine CeO_2 nanoparticles attached to the outer membrane of HepG2 cells. HepG2 cells. SEM images representing the population of (d) untreated HePG2 cells (control), (e) and (f) cells after 24 h incubation with pristine CeO_2 and NH_2-CeO_2 nanoparticles, respectively, each at a concentration of 100 μg/ml.

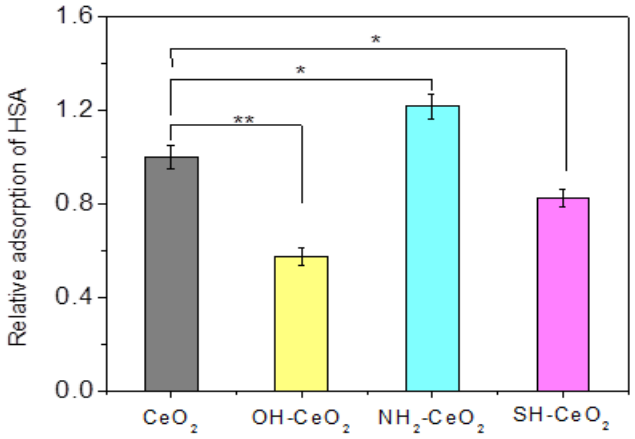

Fig. 5: Relative adsorption of HSA on pristine and functionalized CeO_2 nanoparticles. Statistical significance of the difference in relative protein adsorption is indicated by *$p < 0.01$ and **$p < 0.001$.

3.2 FTIR spectra of the pristine and functionalized CeO_2 nanoparticles

Fourier transform infrared spectroscopy, in absorbance mode, deciphered the vibrational transitions of self-assembled functional groups coordinated to CeO_2 nanoparticle surface nanoparticles [Fig. 2(b)]. Owing to the complex interaction among atoms within the molecules, infrared absorption of the functional groups may vary over a wide range. However, it was found that many functional groups rendered characteristic IR absorption peaks at specific narrow frequency range. The absorption bands around 500 cm^{-1} in all the spectra are produced by CeO_2, which are typical Ce-O stretching vibrations.[23] In the spectrum of the pristine CeO_2 nanoparticles, a broad absorption band at 3450 cm^{-1} is observed, which is correlated to the –OH stretching vibrations, originating from adsorbed water molecules on the surface of CeO_2 nanoparticles.[24] When the surface hydroxyl groups were further activated using H_2O_2, the absorption band around 3450 cm^{-1} was more pronounced, indicating the abundant presence of Ce–OH bonds. Surface modification of CeO_2 nanoparticles with APTES resulted in a characteristic peak at 1560 cm^{-1} in NH_2-CeO_2 that can be corroborated to the $–NH_2$ group present in the grafted aminosilane moiety.[25] The presence of C-N bonds in APTES was manifested in the form of a weak but discernible peak at 1140 cm^{-1}. For MPTMS-modified CeO_2 surface (SH-CeO_2), the S-H stretching vibration in mercaptosilane moiety was manifested in the form of a weak but visible absorption peak at 2530 cm^{-1}. The peaks between 2950 cm^{-1} and 2850 cm^{-1} are due to CH_2 stretching in the silane carbon chains. Finally, successful grafting of the aminosilane or marcaptosilane moieties on CeO_2 surface was substantiated. The appearance of a small peak around 850 cm^{-1}, which represents Ce-O-Si silanolate band, indicates the formation of a covalent binding between the silane ligands and the hydroxyl groups on the nanoparticle surface.[26]

3.3 Hemolytic activity of the nanoparticles

For the nanoparticles to be used as drug-delivery vehicles, they need to be intravenously administered. Since the first physiological system they interact with is blood, interaction of nanoparticles with blood constituents deserves particular attention. In this study, we evaluated the toxicological effects of CeO_2 nanoparticles on human erythrocytes (RBCs) through hemolysis assay. For comparison, the interaction between indigenously synthesized pristine SiO_2 nanospheres and RBC was studied, given that MSN is widely considered as a potential vehicle for the targeted delivery of therapeutics. Vials containing precipitated RBCs after centrifugation, following the incubation of RBC suspensions (in PBS buffer) with various concentrations of SiO_2 and CeO_2 nanoparticles, are presented in Fig. 3. The redness of the supernatant is proportional to the released hemoglobin from the damaged erythrocytes. Hence, the degree of hemolysis, caused by the nanoparticles of given concentration and specific surface functionality, could be correlated to the intensity of red color in the supernatant. In the panels corresponding to pristine SiO_2 and CeO_2 nanoparticles [Fig. 3(a)], the leftmost and rightmost vials represent positive and negative controls, respectively. A dose-dependent hemolysis is apparent from the eventual pallidity of the supernatants (left to right) with the decreasing concentration of the nanoparticles. Further, superior hemocompatibility of CeO_2 nanoparticles, as referred to their SiO_2 counterparts, is evident from visual appearance of the upper two panels. The lower-most panel in Fig. 3(a) represents the influence of surface functionalization of CeO_2 nanoparticles on the degree of hemolysis. In presence of functional groups the hemolytic effect of ceria was significantly reduced. In particular, the aminosilane moieties grafted on the nanoparticle surface remarkably enhanced their hemocompatibility.

Quantitative measurements of the degree of hemolysis were performed by evaluating the absorption peak of

hemoglobin, which was released to the suspension from hemolysed erythrocytes. Figure 3(b) represents comparative data of dose-dependent hemolysis, caused by pristine SiO_2 and CeO_2, respectively. For SiO_2 nanospheres, with an increase in particle concentration from 50 to 1000 µg/ml, the degree of hemolysis increased monotonically from 19–57 %. In comparison, the hemolysis caused by CeO_2 nanoparticles was found to be in the range of 1–12 % when the particle concentration was varied in an identical way. Our experimental data corroborates to the fact that only minimal or no hemolytic activity is observed for cerium oxide nanoparticles.[27]

Surface functionalization of nano ceria had a discernible effect on the degree of hemolysis. Figure 3(c) features a comparative data of hemolysis caused by pristine, hydroxylated and organosilane functionalized CeO_2 nanoparticles in the concentration range of 50–1000 µg/ml. Hemolytic activity of highly hydroxylated CeO_2 surface was examined as these functional groups were created in the process of alkoxysilane grafting. While the activation of surface hydroxyl groups enhanced the hemolytic activity, presence of primary amine or sulfhydryl groups on the surface of the nano-ceria reduced the degree of hemolysis. In particular, CeO_2 nanoparticles grafted with aminosilane showed best hemocompatibility, rendering a mere 5% hemolysis for a particle concentration as high as 1000 µg/ml.

3.4 Cytotoxicity of CeO_2 nanoparticles for HepG2 cells

Measurement of cell viability and proliferation indicates the response of a cell population to external factors, in this case, interaction with nanoparticles in an in vitro setting. The MTT assay measures the cell proliferation rate and conversely, when metabolic events lead to apoptosis or necrosis, the reduction in cell viability. Dose-dependent MTT assays over different exposure times were performed to evaluate short-term and long-term cytotoxicity due to exposure of HepG2 cells to CeO_2 nanoparticles. Toxicity due to short-term exposure was measured after 24 h, while that because of long-term exposure was measured after 6 days. Figure 4 (a) represents the degree of cytotoxicity induced to HepG2 cells by pristine CeO_2 nanoparticles, with a varying dose in the concentration range of 50 to1000 µg/ml. A discernible change in cell viability was observed even at a concentration of 50µg/ml, as the cell survival dropped to 62%, as compared to negative control after 24 h exposure. With an increase in nanoparticle concentration, the cell viability diminished eventually, reaching a value of 35% for CeO_2 concentration of 1000 µg/ml. Further, the long-term exposure data demonstrates that pristine CeO_2 can dramatically affect the viability of HepG2 cells, which plummeted to a value of 19% while exposed to 1000 µg/ml of nanoparticles over a period of 6 days. The observed cytotoxicity with CeO_2 nanoparticles in our study is in agreement with that reported by Marzi et al., who observed that nano-ceria drastically affected the viability of A549 (pulmonary adenocarcinoma) and HepG2 lines at a nanoparticle concentration of 50 µg/Ml.[28] Interestingly, in an in vitro cell culture model of adult rat spinal cord, CeO_2 nanoparticles had shown to promote growth and long-term survival of dissociated adult rat spinal cord neurons.[13] The authors attributed the neuroprotective action of nano-ceria to its auto-regenerative anti-oxidant property. In fact, cerium oxide has potential catalytic and antioxidant activities that resemble to those of catalase and superoxide-dismutase, thereby protecting cells from oxidative stress. This explains why the growth of healthy cells are promoted in presence of CeO_2, up to a certain concentration. On the other hand, CeO_2 can effectively reduce the proliferation of endothelial cells and hence could potentially be used to control the process of angiogenesis.[29] In fact, the anti-angiogenic properties of nanoceria have been demonstrated in preclinical mouse model of ovarian cancer.[30] Reduction of the tumor mass was accompanied by attenuation of angiogenesis and specific apoptosis of vascular endothelial cells. Further, it has been demonstrated that nanoceria selectively bestowed radioprotection to the normal breast cells (CRL 8798) against reactive oxygen species (ROS) compared to the breast cancer cells (MCF 7).[31] Such preferential cytotoxicity of ceria towards cancers cells, over the healthy cells, is intriguing and may be correlated to the pH-dependent redox status of the CeO_2. It has been observed that antioxidant activity CeO_2 is manifested at physiological pH, while its pro-oxidant activity at acidic pH.[32] Noticeably, in solid tumors, the preferential dependence of cancer cells on glycolysis (Warburg effect) leads to a lowering of tumor cell pH.[33] In acidic environments, CeO_2 favorably scavenges superoxide radicals over hydrogen peroxide, causing an accumulation of the latter. On the other hand, in neutral pH (healthy cells), ceria scavenge both.[34]

Since the ROS-modulating activities of nanoceria is attributed to the ability of Ce to switch between Ce^{3+} and Ce^{4+} oxidation states and the compensating oxygen vacancies on the surface,[35] cell viability assays were performed on surface-functionalized CeO_2 as well. Our study had already revealed that grafting of aminosilane moieties on the nanoparticle surface resulted in superior hemo-compatibility. In addition, amino-functionalized nanoparticles have been demonstrated as efficient carriers for the delivery of anticancer drugs.[36] Hence, NH_2-CeO_2 was preferred for the viability studies of HepG2 cells and the results have been compared with that for pristine CeO_2. The amine-modified particles exhibited dose-dependent cytotoxicity for HepG2 cells as well [Figure 4 (b)]. However, for a given concentration and an identical exposure time, the cytotoxic effect was less pronounced for NH_2-CeO_2, as compared to its pristine counterpart. For example, the native CeO_2 showed 53.8 ± 3.5 % cell viability at a concentration of 100 µg/ml for 24 h exposure, whereas the viability increased significantly to 73.8 ± 7.5 when the surface of CeO_2 was modified with APTES. The above results may

be attributed to the bulky aminosilane molecules grafted to the nanoparticle surface, which masked the ROS modulating properties of CeO_2 to a considerable extent. Further, surface functionalization influences the zeta potential of CeO_2, which in turn determines cellular uptake of the nanoparticles through phagocytosis. It is known that the outer leaflet of the cell membrane consists mainly of phosphatidylcholine, the headgroup of which contains a positively charged choline moiety.[37] In spite of overall charge neutrality of phosphatidylcholine, the cationic sites render adsorption of the negatively charged particles. Zeta potential, which is a function of surface charge of the ceria nanoparticles, was found to switch from an appreciable negative value (-18.2 mV) for pristine CeO_2 to a positive value (+14.9 mV) for NH_2-CeO_2 at pH 6.5 [Fig. S2]. The rationale for measuring the Zeta potential of pristine or functionalized CeO_2 in acidic suspension (pH 6.5) is to emulate the microenvironment of cancer cells. The pH of the extracellular space of tumors becomes acidic as the cells employ mechanisms, like lactate and H^+ efflux, to remove acids produced by an enhanced rate of glycolysis within cancer cells.[38] Thus, in the extracellular matrix of carcinoma cell culture, pristine CeO_2 nanoparticles would be negatively charged, which in turn facilitates their adsorption at the positively charged sites of the cell membrane via electrostatic interaction [Figure 4 (c)]. Localized neutralization and a subsequent bending of the plasma membrane favors endocytosis of nanoceria in the cancer cells. On the other hand, due to positive surface charge, NH_2-CeO_2 would have less affinity to be adsorbed on the HepG2 cell surface. Higher cellular uptake of pristine ceria, compared to that of aminosilane-modified nanoparticles, further hikes the intracellular ROS generation beyond the apoptotic threshold and causes higher level of apoptosis of HepG2, when treated the unmodified CeO_2. Scanning electron microscopy images of untreated HepG2 cells, and those incubated with pristine and functionalized CeO_2 nanoparticles for 24 h have been presented in Fig. 4 (d), (e) and (f), respectively. A variation in morphology among the cells treated with pristine or functionalized nanoparticles was apparent. A treatment with 100 µg/ml of pristine CeO_2 for 24 h resulted in reduced viability of the HepG2 cells with occasional blebbing of cell membranes, as a signature of apoptosis. Interestingly, for the same incubation time and for identical concentrations of nanoparticle suspension, the changes in cell population and morphology were less pronounced following the treatment with NH_2-CeO_2 nanoparticles.

From the MTT assay and electron microscopy images it is apparent that aminosilane functionalization quenched the activity of the CeO_2 surface to a significant extent.

3.5 Non-specific protein adsorption

The non-specific adsorption of proteins on the surface of pristine and functionalized CeO_2 were studied by incubating the nanoparticles in HSA, the most abundant protein in human blood. Figure 5 presents the relative degree of HSA adsorption on functionalized CeO_2 surfaces, considering the pristine nanoparticles as reference. With activated hydroxyl groups on the surface, OH-CeO_2 showed about 43% decrease in protein adsorption compared to its pristine counterpart ($p < 0.001$). Interesting properties were observed when aminosilane or marcaptosilane moieties were grafted on ceria nanoparticle surfaces. While an enhanced degree of HSA adsorption was observed with NH_2-CeO_2, the protein binding appeared to be diminished for SH-CeO_2.

Protein adsorption studies have revealed that electrostatic interaction, hydrophobic interaction and specific chemical interactions between protein molecules and the material surface determine the degree of adsorption.[39] It is reported that at physiological pH (~7.4), HSA has net negative charges (-23 per albumin molecule) and the electrostatic forces are dominant over hydrophobic interactions.[40] In our study, the relative adsorption of HSA on pristine and functionalized CeO_2 nanoparticle surfaces can be explained by prevalence of electrostatic interactions. Owing to its more negative surface charge, characterized by a zeta potential value of – 22.9 mV (at pH 6.5), the OH-CeO_2 nanoparticles repels the negatively charged HSA molecules to a greater extent. Subsequently, a decline in surface adsorption of HSA was observed as referred to pristine CeO_2. Enhanced hydrophilicity of the hydroxylated ceria surface further diminished the adsorption of HSA on the nanoparticle surface [Fig. S3 (a) and (b)]. When aminosilane moieties were grafted on CeO_2 surface, an increased adsorption of protein could be observed. The above observation could be attributed to the positive zeta potential (+14.9 mV at pH 6.5) of the amine-terminated surface, which facilitates adsorption of negatively charged HSA molecules by columbic interaction. Additionally, hydrophobicity of the aminosilane-grafted surface (water contact angle of 93±2o), promoted HSA adsorption on NH_2-CeO_2 [Fig. S3(c)]. Interestingly, HSA adsorption on MPTMS-modified CeO_2 surface was less as compared to their pristine counterpart and may be attributed to the negatively charged surface of SH-CeO_2. With a zeta potential of –7.6 mV, the thiolated surface exerted a repulsion effect, which surpassed the hydrophobic interaction for protein binding.

4. CONCLUSIONS

Even in its pristine form, cerium oxide offers superior biocompatibility as referred to silica, the present gold standard. Interactions of ceria with biological cells are further tweaked by modifying the nanoparticle surface either by activating hydroxyl groups or by grafting aminosilane or marcaptosilane moieties. The degree of hemolysis was significantly reduced when CeO_2 surface was modified with aminosilane. However, the pro-oxidant therapeutic activities of unmodified CeO_2 was found to be partially quenched when HepG2 cells were treated with an identical dose amine-functionalized nanoparticles, thus associating the ROS-modulating properties of ceria with the presence of Ce^{3+} and the

corresponding oxygen vacancies on the surface. When it comes to protein adsorption, electrostatic interaction was found to be predominant over hydrophobic or van der Walls force. Though aminosilane treatment enhances adsorption of HSA on ceria surface, owing to better hemocompatibility of HSA-coated particles, it is an advantageous aspect for injectable ceria suspension. Taking together the facts it can be inferred that with the deployment of prudent surface functionalization strategies, customized drug-delivery cargos or theranostic systems can be developed based on cerium oxide.

AKNOWLEDGEMENT

The authors gladly acknowledge the guidance provided by Prof. M.K. Mitra, Retired Professor, Jadavpur University, Kolkata and Dr. U.K. Biswas, N.R.S Medical College and Hospital, Kolkata throughout the work.

REFERENCES

1. Paanyam J, Labhasetwar V. (Biodegradable nanoparticles for drug and gene delivery to cells and tissue). Adv Drug Deliv Rev, 2003; 55(1): 329-47.
2. Kresge CT, Leonowicz ME, Roth W J, Vartuli JC, Beck JS. (Ordered mesoporous molecular sieves synthesized by a liquid-crystal template mechanism). Nature, 1992; 359(1): 710-712.
3. Vallet-Regi M, Ramila A, del Real RP, Perez-Pariente J. (new property of MCM-41: drug delivery system). Chem Mater, 2001; 13(1): 308.
4. Lai CY, Trewyn BG, Jeftinija K, Xu S, Jeftinija S, Lin VS. (A Mesoporous Silica Nanosphere-Based Carrier System with Chemically Removable CdS Nanoparticle Caps for Stimuli-Responsive Controlled Release of Neurotransmitters and Drug Molecules). J A Chem Soc, 2003; 125(1): 4451.
5. Lin YS, Haynes CL. (Impacts of mesoporous silica nanoparticle size, pore ordering, and pore integrity on hemolytic activity). J Am Chem Soc, 2010; 132(1): 4834-4842.
6. Datta A, Dasgupta S, Mukherjee S. (Modifications of nano-titania surface for in vitro evaluations of hemolysis, cytotoxicity, and nonspecific protein binding). J Nanopart Res, 2017; 19(1): 142.
7. Briggs RT, Drath DB, Karnovsky ML, Karnovsky MJ. (Localization of NADH oxidase on the surface of human polymorphonuclear leukocytes by a new cytochemical method). J Cell Biol, 1975; 67(1): 566-86.
8. Eguchi K, Setoguchi T, Inoue T, Arai H. (Electrical properties of ceria-based oxides and their application to solid oxide fuel-cells). Solid State Ion, 1992; 52(1): 165–72.
9. Tsunekawa S, Sivamohan R, Ohsuna T, Kasuya A, Takahashi H, Tohji K. (Ultraviolet absorption spectra of CeO_2 nano-particles). Mater Sci Forum, 1999; 315–317(1): 439–45.
10. Izu N, Shin W, Matsubara I, Murayama N. (Development of resistive oxygen sensors based on cerium oxide thick film). J Electroceramics, 2004; 13(1): 703–6.
11. Xia T, Kovochich M, Liong M, Mädler L, Gilbert B, Shi H, Yeh JI, et al. (Comparison of the Mechanism of Toxicity of Zinc Oxide and Cerium Oxide Nanoparticles Based on Dissolution and Oxidative Stress Properties). ACS Nano, 2008; 2(1): 2121–2134.
12. Niu J, Azfer A, Rogers LM, Wang X, Kolattukudy PE. (Cardioprotective effects of cerium oxide nanoparticles in a transgenic murine model of cardiomyopathy). Cardiovasc Res, 2007; 73(1): 549–559.
13. Das M, Patil S, Bhargava N, Kang J-F, Riedel LM, Seal S, Hickman JJ. (Auto-catalytic Ceria Nanoparticles Offer Neuroprotection to Adult Rat Spinal Cord Neurons). Biomaterials, 2007; 28(1): 1918–1925.
14. Linse S, Cabaleiro-Lago C, Xue WF. (Nucleation of protein fibrillation by nanoparticles). PNAS, 2007; 104(1): 8691–8696.
15. Ehrlich V, Darroudi F, Uhl M, Steinkellner S, Zsivkovits M, Knasmeuller S. (Fumonisin B1 is genotoxic in human derived hepatoma (HepG2) cells). Mutagenesis, 2002; 17(1): 257-260.
16. Owens DE, Peppas NA. (Opsonization, biodistribution, and pharmacokinetics of polymeric nanoparticles). Int J Pharm, 2006; 307(1): 93-102.
17. Zhang Y, Kohler N, Zhang M. (Surface modification of superparamagnetic magnetite nanoparticles and their intracellular uptake). Biomaterials, 2002; 23(1): 1553–61.
18. Zhao Y, Sun X, Zhang G, Trewyn B. (Slowing II, Lin V. Interaction of mesoporous silica nanoparticles with human red blood cell membranes: size and surface effects). ACS Nano, 2011; 5(1): 1366–1375.
19. Yildirim A, Ozgurab E, Bayindir M. (Impact of mesoporous silica nanoparticle surface functionality on hemolytic activity, thrombogenicity and non-specific protein adsorption). J Mater Chem B, 2013; 1(1): 1909–1920.
20. Mossman T. (Rapid Colorimetric Assay for cellular growth and survival: Application to proliferation and Cytotoxicity assays). J. Immunol. Methods, 1983; 65(1): 55-63.
21. Grainger D W, Jones C F. (In Vitro Assessments of Nanomaterial Toxicity). Adv Drug Deliv Rev, 2009; 61(1): 438−456.
22. He Q, Zhang J, Shi J, Zhu Z, Zhang L, Bu W, et al. (The effect of PEGylation of mesoporous silica nanoparticles on nonspecific binding of serum proteins and cellular responses). Biomaterials, 2010; 31(1): 1085–1092.
23. Palard M, Balencie J, Maguer A, Hochepied J-F. (Effect of hydrothermal ripening on the photoluminescence properties of pure and doped cerium oxide nanoparticles). Mater Chem Phys, 2010; 120(1): 79-88.

24. Niu F, Zhang D, iShib L, He X, Li H, Mai H, et al. (Facile synthesis, characterization and low-temperature catalytic performance of Au/CeO_2 nanorods). Mater Lett, 2009; 63(1): 2132-2135.
25. Dowding JM, Dosani T, Kumar A, Seal S, Self WT. (Cerium oxide nanoparticles scavenge nitric oxide radical ($^{\cdot}NO$)). ChemComm, 2012; 48(1): 4896–4898.
26. Xue Y, Luan Q, Yang D, Yao X, Zhou K. (Direct evidence for hydroxyl radical scavenging activity of cerium oxide nanoparticles). J Phys Chem, 2011; 115(1): 4433–4438.
27. Kotsuruba AV, Kopjak BS, Sagach VF, Spivak MY. (Cerium oxide nanoparticles restore erythrocyte stability to acid hemolysis in old rats). Int J Physiol Pathophysiol, 2015; 6(1): 339-346.
28. Marzi LD, Monaco AM, Lapuente J, Ramos DB, Borrás M, Gioacchino MD, Santucci S, Poma A. (Cytotoxicity and Genotoxicity of Ceria Nanoparticles on Different Cell Lines in Vitro). Int J Mol Sci, 2013; 14(1): 3065-3077.
29. Lord MS, Tsoi B, Gunawan C, Teoh WY, Amal R, Whitelock JM. (Anti-angiogenic activity of heparin functionalised cerium oxide Nanoparticles). Biomaterials, 2013; 34(1): 8808–8818.
30. Giri S, Karakoti A, Graham RP, Maguire JL, Reilly CM, Seal S, et al. (Nanoceria: A Rare-Earth Nanoparticle as a Novel Anti-Angiogenic Therapeutic Agent in Ovarian Cancer). PLoS One, 2013; 8(1): e54578.
31. Tarnuzzer RW, Colon J, Patil S, Seal S. (Vacancy engineered ceria nanostructures for protection from radiation-induced cellular damage). Nano Lett, 2005; 5(1): 2573–2577.
32. Asati A, Santra S, Kaittanis C, Nath S, Perez JM. (Oxidase-Like Activity of Polymer-Coated Cerium Oxide Nanoparticles). Angew Chem Int, 2009; 48(1): 2308–2312.
33. Shamim U, Hanif S, Albanyan A, Beck FW, Bao B, Wang Z, et al. (Resveratrol-induced apoptosis is enhanced in low pH environments associated with cancer). J Cell Physiol, 2012; 227(4): 1493-500.
34. Marzi LD, Monaco A, Lapuente JD, Ramos D, Borras M, Gioacchino MD, et. al. (Cytotoxicity and Genotoxicity of Ceria Nanoparticles on Different Cell Lines in Vitro). Int J Mol Sci, 2013; 14: 3065-3077.
35. Celardo I, Nicola MD, Mandoli C, Pedersen JZ, Traversa E, Ghibelli L. (Ce^{3+} Ions Determine Redox-Dependent Anti-apoptotic Effect of Cerium Oxide Nanoparticles). ACS Nano, 2011; 6(1): 4537-4549.
36. He Y, Luo L, Liang S, Long M, Xu H. (Amino-functionalized mesoporous silica nanoparticles as efficient carriers for anticancer drug delivery). J Biomater Appl, 2017; 32(4): 524-532.
37. Cooper GM. The Cell: A Molecular Approach. 2nd edition. Sunderland (MA): Sinauer Associates, 2000.
38. Damaghi M, Wojtkowiak JW, Gillies RJ. (pH sensing and regulation in cancer). Front Physiol, 2013; 4(1): 370.
39. Sigal GB, Mrksich M, Whitesides GM. (Effect of surface wettability on the adsorption of proteins and detergents). JACS, 1998; 120(14): 3464–3473.
40. Salgin S, Takac S, Ozdamar T H. (Adsorption of bovine serum albumin on polyether sulfone ultrafiltration membranes: determination of interfacial interaction energy and effective diffusion coefficient). J Membr Sci, 2006; 278(1–2): 251–60.

Supplementary Information

IN-VITRO ASSESSMENT OF CERIUM OXIDE NANOPARTICLES AS PROMISING DRUG-DELIVERY VEHICLES: INFLUENCE OF SURFACE FUNCTIONALIZATION

Aparna Datta[1*], Deblina Majumder[2], Preetam Guha Ray[2], Somenath Roy[2], Sayantan Dasgupta[3] Siddharta Mukherjee[4]

[1]School of Pharmacy, Sharda University, Knowledge Park III, Greater Noida 201310, Uttar Pradesh, India.
[2]Sensor and Actuator Division, CSIR-Central Glass and Ceramic Research Institute, 196, Raja S.C. Mullick Road, Kolkata 700032 India.
[3]Department of Biochemistry, NRS Medical College and Hospital, 138 A.J.C. Bose Road, Kolkata 700014, West Bengal, India.
[4]Department of Metallurgical and Material Engineering, Jadavpur University, 188, Raja S.C. Mullick Road, Kolkata 700032, West Bengal, India.

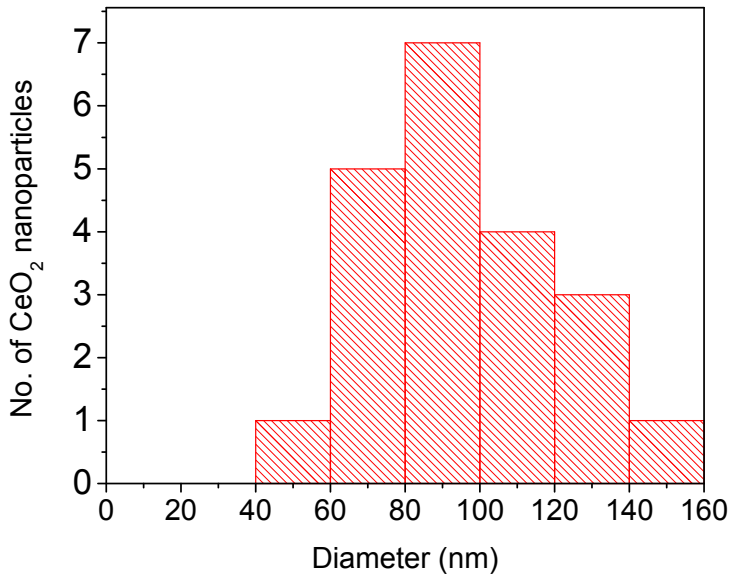

Fig. S1: Particle size distribution for CeO_2

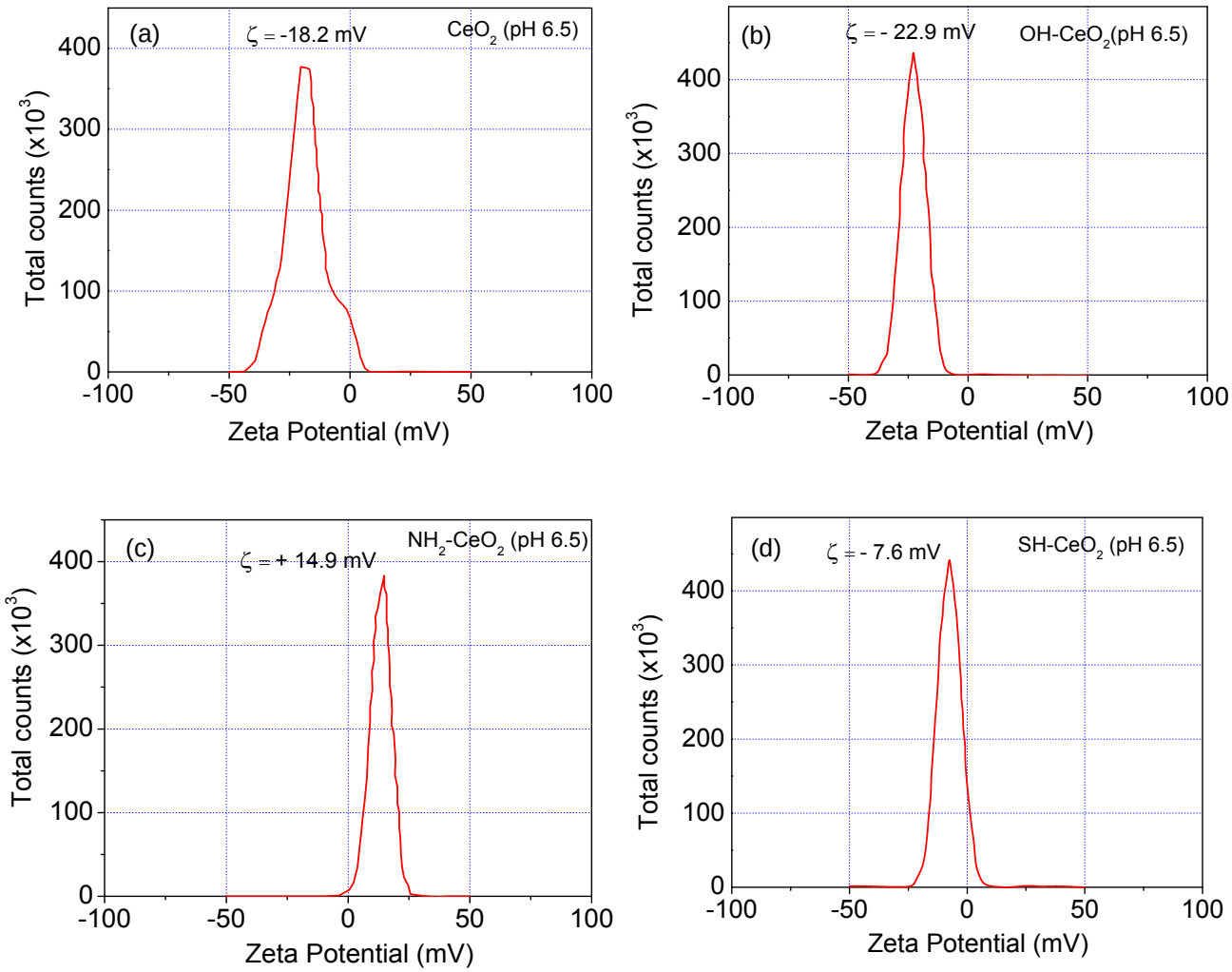

Fig. S2: Zeta potential of cerium oxide nanoparticles at pH 6.5. **(a)** Pristine CeO_2, **(b)** OH- CeO_2, **(c)** NH_2-CeO_2 and **(d)** SH- CeO_2

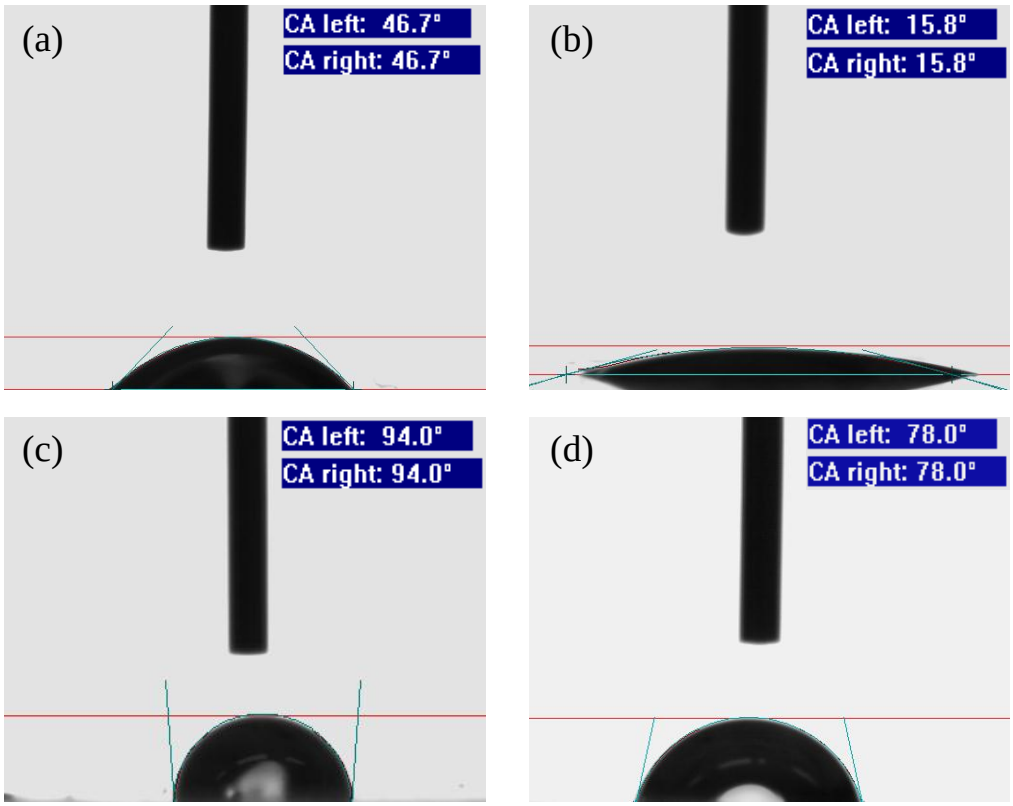

Fig. S3: Water contact angle on cerium oxide-coated glass surface. **(a)** Pristine CeO_2, **(b)** OH-CeO_2, **(c)** NH_2- CeO_2 and **(d)** SH- CeO_2